The diffraction part of

Oxidation of some Late Transition Metal Surfaces: Structural studies from UHV to Atmospheric Pressure

PhD Thesis

Johan Gustafson
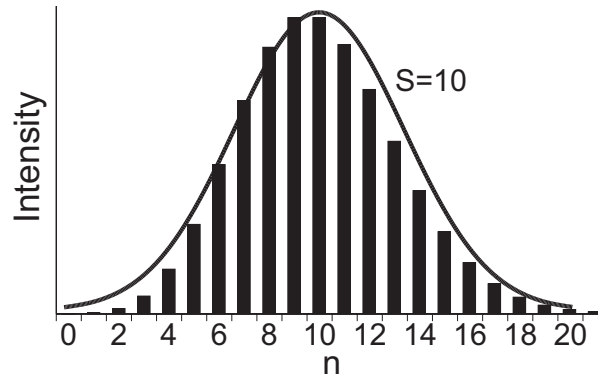Div. of Syncrotron Radiation Research
Lund University

Figure 3.5: The Poisson distribution for $S = 10$, where $S = P(1)/P(0)$. The number of phonons created in a photoemission process follows this distribution, and we see that at this relatively large S, the distribution is very close to Gaussian, which is described by the solid line. Thus, in most metals, the phonon creation shows up in the photoemission spectrum as a Gaussian broadening of the peaks.

the phonons also makes it impossible to resolve the different components, and the result is simply a Gaussian broadening of the original photoemission peak, described by

$$I_G(E) = I_0 e^{-\frac{\ln 2 (E_0 - E)^2}{\sigma^2/4}} \tag{3.7}$$

where σ is the Gaussian FWHM.

Finally, all measurements include a built in uncertainty and there is always some degree of disorder in the sample. Most often this results in a close to random distribution of the measured data, thus simply adding to the Gaussian broadening.

The Fitting Procedure

The final line shape is given by a convolution of the three different broadening contributions and if several components – corresponding e.g. to different chemical surroundings or resolved vibrations – are present the total line shape is achieved by the sum of them. The actual analysis is performed by a computer program such as FitXPS [32]. As input is used a first guess on E_0, I_0, Γ, α and σ for each peak. These fitting parameters are then automatically varied in the search for a total line shape as close to the measured spectrum as possible. The result then has to be checked so that it makes physical sense, and if needed one can redo the fit after adding constraints on the fitting parameters.

3.2   Diffraction Methods

The standard way to determine periodic structures is to use some kind of diffraction method. The result is a map of the so-called reciprocal lattice, which is a Fourier transform of the real lattice and thus reflects the periodicity of the sample. In this thesis, two different diffraction methods are used, namely low energy electron diffraction (LEED) [33] and surface x-ray diffraction (SXRD) [34, 35].

In addition to different methods, one often distinguishes between so-called qualitative and quantitative diffraction measurements. While a qualitative study aims at finding the main features of a structure, like the cell dimensions and presence of different phases, the goal of a quantitative study is a detailed description of the atomic positions. My work with diffraction has been almost exclusively qualitative, and therefore this chapter will only briefly touch upon quantitative measurements.

The basic theory of diffraction methods in general [8, 9] and surface diffraction in particular [14, 34] is covered in 3.2.1 and 3.2.2 respectively, while the specific properties of each method are covered in 3.2.3 and 3.2.4

3.2.1 Basic Diffraction Theory

The basics of all diffraction experiments are two observations from wave mechanics:

- When a wave interacts with a spherical object, it is scattered in all directions from the object.

- Two waves that meet will interfere with each other to form one wave with larger amplitude where they are in phase (constructive interference), and smaller amplitude where they are out of phase (destructive interference).

In a crystal the atoms act as scatterers, and waves scattered by different atoms will interfere with each other. Assuming that the scattering is elastic, this will yield an interference pattern with information about the atomic structure. Fig. 3.6 shows an incoming wave that is scattered by two atoms separated by a lattice vector $\mathbf{R} = m_1\mathbf{a}_1 + m_2\mathbf{a}_2 + m_3\mathbf{a}_3$, and a detector measuring the scattered intensity in a certain direction. In order to have the beams in phase, and thus obtain constructive interference, the path difference[i], PD, must be an integer number of wavelengths, i.e. $PD = n\lambda$, where n is any integer. From the geometry in Fig. 3.6, the requirement for constructive interference is then given by

$$n\lambda = PD = R\cos\theta + R\cos\theta' \tag{3.8}$$

where $R = |\mathbf{R}|$ is the distance between the atoms. In order to have full constructive interference in a whole crystal, equation 3.8 has to be fulfilled for any possible $\mathbf{R}$.
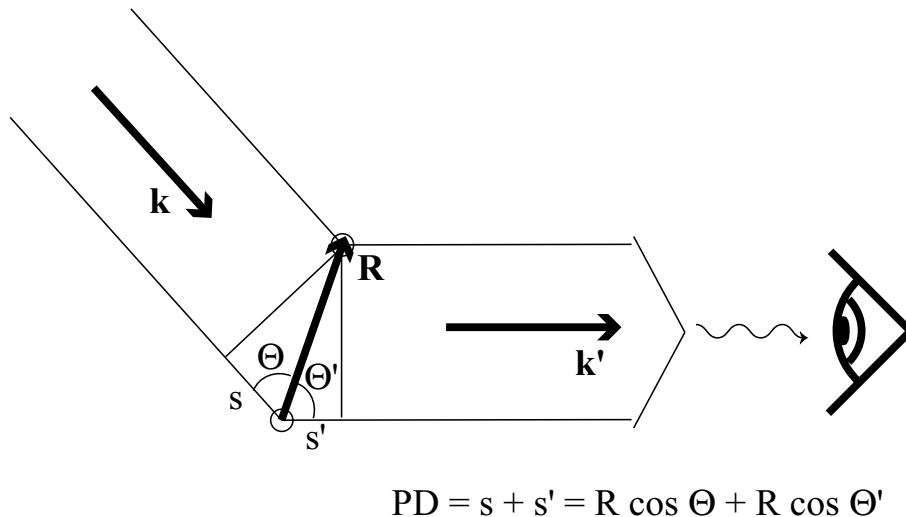

$$PD = s + s' = R\cos\Theta + R\cos\Theta'$$

Figure 3.6: Illustration of a diffraction experiment with an incoming wave that is scattered by two scatterers. Beams scattered by different scatterers in the same direction interfere constructively if their path difference, PD, is a multiple of the wavelength.

---

[i]The path difference is the difference in the distance the two beams have to travel from the source to the observer via the scatterers.

It is now convenient to describe the wave by its wave vector, $\mathbf{k}$, defined as pointing in the direction of propagation and of length, $k = |\mathbf{k}| = \frac{2\pi}{\lambda} = \frac{p}{\hbar}$, proportional to the momentum, p, of the wave particle. In Fig. 3.6 $\mathbf{k}$ and $\mathbf{k}'$ are the wave vectors of the incoming and outgoing wave respectively, and as mentioned above the scattering is assumed to be elastic, so that $|\mathbf{k}| = |\mathbf{k}'| = k$. Using this, the condition for constructive interference can be rewritten as

$$\frac{\mathbf{R} \cdot \mathbf{k}'}{k} - \frac{\mathbf{R} \cdot \mathbf{k}}{k} = \frac{\mathbf{R} \cdot \mathbf{\Delta k}}{k} = PD = n\lambda = n\frac{2\pi}{k}$$
$$\mathbf{R} \cdot \mathbf{\Delta k} = 2\pi n \tag{3.9}$$

where $\mathbf{\Delta k} = \mathbf{k}' - \mathbf{k}$, i.e. the momentum change during scattering.

The Reciprocal Lattice

Here the so-called reciprocal lattice, corresponding to the atomic lattice above, is defined by basis vectors, $\mathbf{b}_1$, $\mathbf{b}_2$ and $\mathbf{b}_3$, as

$$\mathbf{b}_i \cdot \mathbf{a}_j = \delta_{ij} 2\pi. \tag{3.10}$$

This lattice is the Fourier transform of the real lattice and thus well defined by the latter as a periodic array of points in reciprocal space[ii]. An arbitrary reciprocal lattice vector, $\mathbf{G}$, is described by $\mathbf{G} = q_1\mathbf{b}_1 + q_2\mathbf{b}_2 + q_3\mathbf{b}_3$, where q_1, q_2 and q_3 are integers. Note, however, that $\mathbf{b}_1$, $\mathbf{b}_2$ and $\mathbf{b}_3$ span all of reciprocal space, so that any reciprocal vector can be expressed in this basis, although only those with integer coordinates are vectors belonging to the lattice. E.g. one can express $\mathbf{\Delta k} = (h\mathbf{b}_1 + k\mathbf{b}_2 + l\mathbf{b}_3)$ in this basis and develop equation 3.9.

$$2\pi n = \mathbf{R} \cdot \mathbf{\Delta k} = (m_1\mathbf{a}_1 + m_2\mathbf{a}_2 + m_3\mathbf{a}_3) \cdot (h\mathbf{b}_1 + k\mathbf{b}_2 + l\mathbf{b}_3)$$
$$= (m_1 h + m_2 k + m_3 l)2\pi \tag{3.11}$$
$$(m_1 h + m_2 k + m_3 l) = n$$

As mentioned above, in order to have full constructive interference, this has to be true for all possible real lattice vectors $\mathbf{R}$. This requires that h, k and l are all integers, which turns $\mathbf{\Delta k}$ into a reciprocal lattice vector. The other way around one has

$$\mathbf{R} \cdot \mathbf{G} = (m_1\mathbf{a}_1 + m_2\mathbf{a}_2 + m_3\mathbf{a}_3) \cdot (q_1\mathbf{b}_1 + q_2\mathbf{b}_2 + q_3\mathbf{b}_3) = (m_1 q_1 + m_2 q_2 + m_3 q_3)2\pi \tag{3.12}$$

which, since the last parenthesis is an integer (a sum of products of integers), fulfills constructive interference as well with $\mathbf{\Delta k} = \mathbf{G}$.

It is now shown that if and only if the change in wave vector during the scattering process is a reciprocal lattice vector, one will obtain constructive interference, i.e. if

$$\mathbf{\Delta k} = \mathbf{G}. \tag{3.13}$$

The points in this three-dimensional reciprocal lattice are often referred to as Bragg points.

The idea of a diffraction experiment is to scan reciprocal space in order to map out the reciprocal lattice, which can be translated into the real lattice. How to perform this translation is defined by equation 3.10. Provided that the real lattice is described as shown on page 6 (with $\mathbf{a}_1$ and $\mathbf{a}_2$ defining the surface lattice and $\mathbf{a}_3$ perpendicular to the surface plane), the reciprocal lattice can be described by basis vectors with the same relative angles as the real ones. Their relative lengths, on the other hand, are inverted.

[ii]The dimension of reciprocal space is momentum, and it is therefore often referred to momentum space. Thus a wave vector is also a reciprocal vector.

3.2.2   Surface Diffraction

In the discussion above the crystal is assumed to be infinitely large, which is a valid approximation for directions parallel to the surface. But the penetration depth of the beam is finite, which breaks the periodicity perpendicular to the surface. This affects the Fourier transform so that the reciprocal lattice, and thus the interference pattern, does not only consist of delta-functions.

Fig. 3.7 shows a simulation of the intensity variations along a row of reciprocal lattice points perpendicular to the surface, for different penetration depths. The two extremes, scattering in a single layer and an infinite crystal, are presented in Fig. 3.7a. Since the radiation scattered in a single layer does not interfere with any other radiation, the result is a constant intensity distribution, as shown by the dashed line[iii]. Since our goal with the diffraction experiment is to find surface specific information, this is exactly the intensity we are searching for. Therefore we use it as unit for the intensity also in the other cases. The infinite crystal is not simulated, but should according to the theoretical discussion above correspond to delta-functions that are infinitely high and narrow. This is presented as the solid lines in Fig. 3.7a, and the intensity is concentrated to the integer values of l, corresponding to the Bragg points.

Simulations corresponding to typical standard x-ray diffraction (XRD), SXRD and LEED experiments are shown in Fig. 3.7b-d, with penetration depths in the order of 1 μm, 10 nm and 10 Å respectively. For the simulation of standard x-ray diffraction we find a ratio between the signals from the surface and in the peaks of about 10^{-7}, which is so small that the infinite crystal approximation is valid, and these measurements are not suitable for surface studies. With decreasing penetration depth we find an increasing surface to peak signal ratio, as expected. At conditions similar to those for SXRD[iv] (Fig. 3.7c) it has increased to $\sim 0.1\%$, which is sufficient for meaningful measurements, and for LEED (Fig. 3.7d) the surface and peak signals are directly comparable.

Crystal Truncation Rods and In-Plane Diffraction

An important difference between an infinite crystal (Fig. 3.7a) and one with a surface (Fig. 3.7b-d) is the intensity in the minima in-between the Bragg points. In the latter case the intensity never reaches 0, but the intensity is smeared out to form so-called Crystal Truncation Rods (CTRs), connecting Bragg points stacked perpendicular to the surface.

This means that in the search for the surface lattice, which is a major goal in diffraction studies of surfaces, one does not have to consider the l value. As long as h and k are integers one will find some scattered intensity, and the condition for which one will obtain constructive interference (equation 3.13) will, for in-plane diffraction, change into

$$\Delta \mathbf{k}_{||} = \mathbf{G}_{\mathrm{s}} = h\mathbf{b}_1 + k\mathbf{b}_2. \qquad (3.14)$$

where $\Delta \mathbf{k}_{||}$ is the component of $\Delta \mathbf{k}$ that is parallel to the surface plane, and $\mathbf{G}_{\mathrm{s}}$ is a reciprocal surface lattice vector. Note, however, that in cases like a (553) surface, where the distance between the Bragg points along the CTRs is long, and if the surface is not absolutely perfect, the intensity in the minima may still be very low, and it might be a good idea to avoid these l values.

The CTRs are also used in quantitative surface diffraction measurements, since their shapes are very sensitive to surface rearrangements and relaxations [35]. For example, Fig. 3.8 shows a simulated CTR of a crystal with a 5% inwards relaxation of the top layer, with a penetration depth corresponding to a LEED measurement. The contrast to the bulk termination in Fig. 3.7d is striking and by

---

[iii]The scattering is here assumed to be uniform, i.e. only the interference changes the intensity.

[iv]In this example the penetration depth is 1% of that of standard XRD, due to a grazing incidence angle of $\sim 1°$.
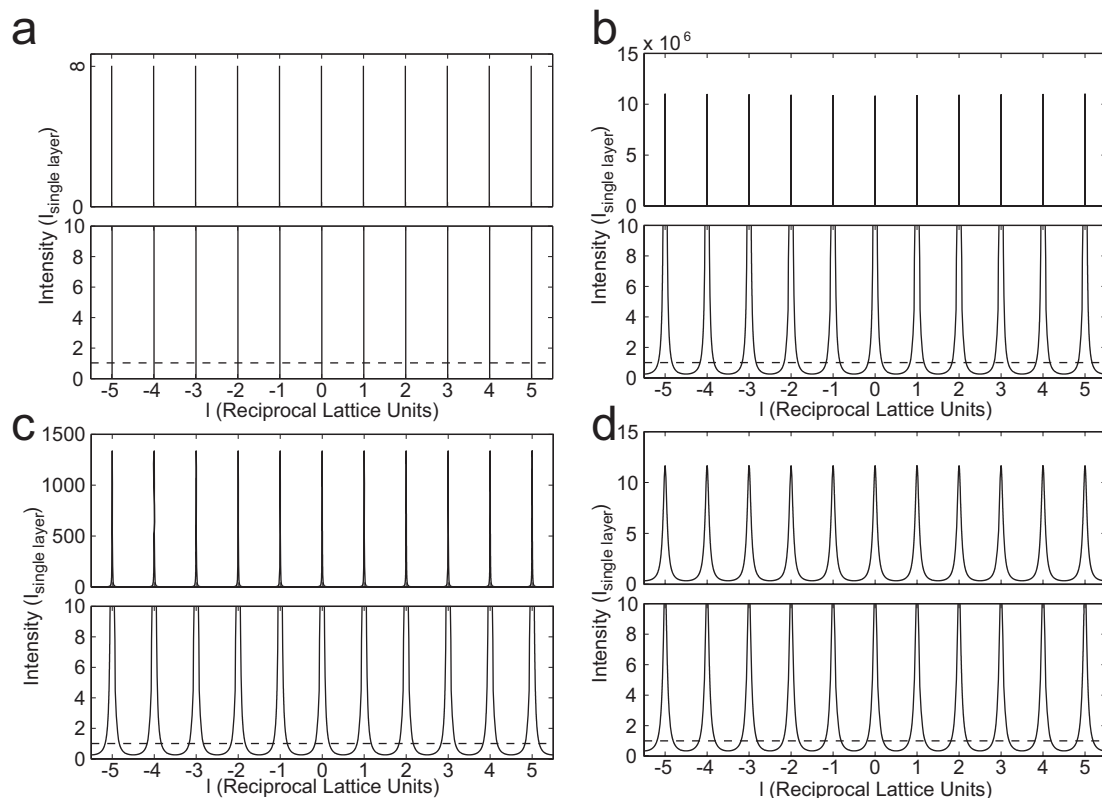
Figure 3.7: Simulated CTRs corresponding to different penetration depths, illustrating the effect of a surface on a diffraction signal. a) In the case of an infinite crystal (solid lines) the intensity is concentrated to delta functions at integer l-values, while for a single layer (dashed), the intensity is constant with l. b-d) For a finite crystal, with a surface, the intensity is spread out along the direction perpendicular to the surface. With a penetration depth corresponding to standard XRD (b), the relative intensity in-between the Bragg points or from a single layer is experimentally negligible. With decreasing penetration depth the relative surface signal increases to a significant level for conditions similar to SXRD (c), and is directly comparable to the bragg point intensities in the case of LEED (d).

fitting a simulation to measured CTRs it is possible to determine structures, including relaxation, very accurately [34, 35].

3.2.3   Low Energy Electron Diffraction

In LEED the fact that electrons may be treated as waves is used. This idea was put forward by de Broglie, who proposed that the corresponding wave length is given by $\lambda = \frac{h}{p}$, where h is the Planck's constant and p is the momentum of the electron. The wave nature of electrons was confirmed in the very first LEED experiment by Davisson and Germer in 1927 [33, 36]. The short mean free path of low energy electrons makes LEED a very surface sensitive method. The basic use, as well as the experimental setup, is also relatively simple. Consequently almost every surface science laboratory includes a LEED equipment, which is used to check the periodicity of the surface before starting more thorough measurements.

The LEED optics, i.e. the experimental setup, is shown schematically in figure 3.9. An electron gun with variable accelerating potential provides a monoenergetic electron beam, which is sent onto the sample surface, scattered backwards and detected on the fluorescent screen (S). This screen lights
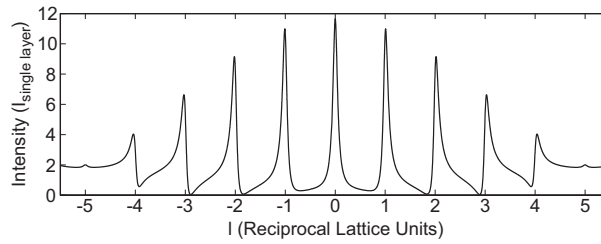
Figure 3.8: A simulated CTR corresponding to a LEED measurement on a crystal with 5% inwards surface layer relaxation.

up when hit by high energy electrons, and is therefore put on a high positive potential (V_S) in order to give the scattered low energy electrons a sufficient extra energy. In order to detect elastically scattered electrons only, a grid (G2) is set to a negative potential of the same size as the accelerating potential. Thus only those electrons that have kept all their energy will be able to pass this grid and all inelastically scattered electrons are sorted away. This field should, however, not affect the directions of the scattered electrons, and therefore a grounded grid (G3) is inserted on the sample side of G2. Similarly the rest of the optics is isolated from the large field of the screen by G1, which is grounded as well.
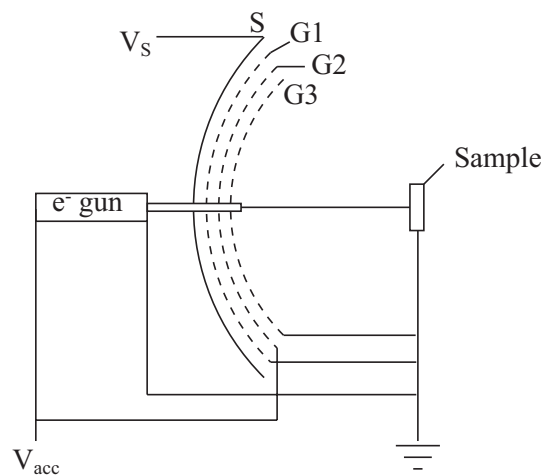

Figure 3.9: Schematic picture of the LEED optics. An electron gun sends electrons onto the sample, where they are scattered backwards. In the directions with constructive interference, intensity maxima will be detected on the fluorescent screen, S. A number of grids are placed between the sample and the screen to make sure that only elastically scattered electrons are detected and that the directions of the electrons will not be affected by any electric fields.

Fig. 3.10 shows the situation in reciprocal space, with a wave vector $\mathbf{k}$ coming in perpendicular to the reciprocal surface lattice, and scattered waves $\mathbf{k}'_i$ going out of the surface. Since $\mathbf{k}$ is perpendicular to the surface $\mathbf{k}_{||} = 0$, and therefore $\Delta\mathbf{k}_{||} = \mathbf{k}'_{||} - \mathbf{k}_{||} = \mathbf{k}'_{||} = \mathbf{G}_s$, for constructive interference. Thus, the directions of the outgoing wave vectors must be such that their projections on the lattice reaches from one reciprocal lattice point to another. In Fig. 3.10 e.g. $\mathbf{k}'_{2||} = 2\mathbf{b}$ and one will get a diffraction peak in the direction of $\mathbf{k}'_2$, which is observed as a bright spot on the fluorescent screen of the LEED optics. As seen from Fig. 3.10, if the screen is observed from the top, one will simply observe a picture of the reciprocal lattice scaled into real space units [37].

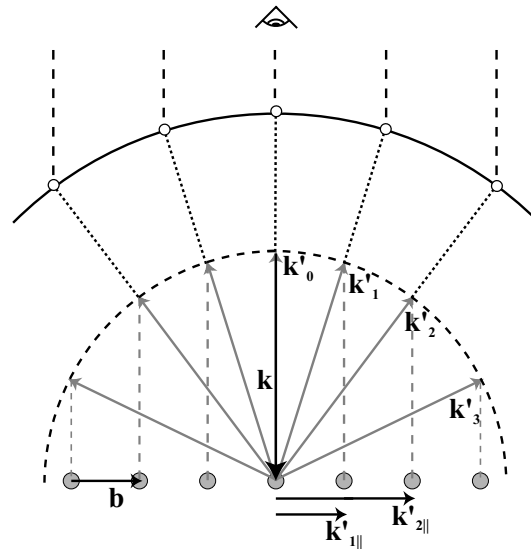As an example, Fig. 3.11a shows the LEED pattern from a clean Rh(111) surface. Its surface lattice

Figure 3.10: The LEED experiment. A wave vector **k** is coming in along the surface normal. In directions where the projection of the scattered wave vector on the surface, $\mathbf{k}'_{||}$, is a reciprocal lattice vector, constructive interference will be obtained and intensity maxima detected on the spherical screen. If this is observed from the top one will see an image of the reciprocal lattice scaled into real units.

is hexagonal, and so is, as seen, the corresponding reciprocal lattice.
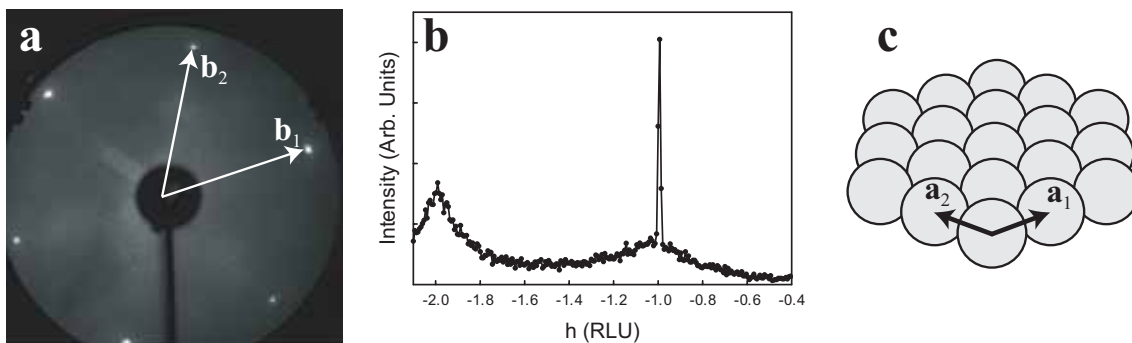

Figure 3.11: LEED and SXRD from the clean Rh(111) surface. a) The LEED pattern shows the hexagonal reciprocal lattice corresponding to the hexagonal surface structure shown in c. b) SXRD scan along the negative h-direction in $k = 0$ and $l = 0.3$. Since l is not an integer, we do not measure the Bragg points, but we still find intensity at integer h-values due to the diffuse scattering of the CTRs.

3.2.4 Surface X-ray Diffraction

The x-rays used in SXRD interact very weakly with matter, and are not significantly affected by the presence of a gas. This makes it one of the few methods available for detailed surface structure determination in high pressures. Using SXRD it is e.g. possible to follow an oxidation process in a "live" mode, and monitor under what conditions different phases are formed and stable, which plays a crucial role in this thesis.

Unfortunately, the benefits of SXRD do not come without complications. The long mean free path of x-rays leads to large penetration depths, and consequently standard XRD is used for bulk-

structure determinations and the surface contribution to the measured signal is negligible. Thus in order to enable surface studies by XRD, the surface sensitivity has to be increased, which is achieved in a number of steps.

First of all, the measurements are performed in parts of reciprocal space, where the intensity corresponding to the bulk is low. For instance, the reciprocal lattice of a surface reconstruction most often includes points in non-integer h and k values, where the bulk intensity is limited to background noise. But if the surface intensity is too low relative to the bulk, as in standard XRD, the signal-to-noise ratio will be too small for allowing surface investigations. By using grazing incidence with an angle of $\sim 1°$ between the incoming beam and the surface, the penetration depth is geometrically decreased by about two orders of magnitude. As described in Fig. 3.7c, this increases the surface signal relative to that of the bulk, and hence also as compared to the noise, to a significant level. In order to increase the surface sensitivity even more, the angle of incidence is often set equal to the critical angle for total reflection [34]. Using grazing incidence, however, mainly decreases the noise level, and the intensity scattered by the surface is still low. Consequently most SXRD studies are performed using synchrotron radiation sources, in order to increase the total intensity.

It is often convenient to include also the substrate lattice in the measurements, either as reference or in order to study the properties of the substrate surface. This can preferably be done somewhere along a CTRs where the intensity is suitable. As shown in Fig. 3.8, a considerable amount of information is also contained in the shape of the CTRs. If, for instance, the surface gets rough due to some reaction, it is identified by a decrease of the intensity in the minima of the CTRs [38].

The Measurement

The diffraction measurement can be illustrated by the so-called Ewald sphere shown in Fig. 3.12 [9]. The incoming wave vector, $\mathbf{k}$, is drawn such that it points at a reciprocal lattice point and the outgoing lattice vector, $\mathbf{k}'$, is placed sharing the same starting point. $\mathbf{k}'$ can then reach the points in reciprocal space, that lie on a sphere of radius k around the starting point, and by placing a detector in the direction of $\mathbf{k}'$, the corresponding intensity can be measured. The momentum change $\mathbf{\Delta k}$ is shown as the vector between the endpoints of $\mathbf{k}$ and $\mathbf{k}'$, and in the case that $\mathbf{\Delta k}$ is a reciprocal lattice vector, constructive interference, and thus an intensity peak, is obtained.

With the geometry in Fig 3.12a, 5 different lattice points (including the (0,0) point) can be found by moving the detector. In order to measure other parts of reciprocal space, the sample, and thus the reciprocal lattice, is rotated such that new points fall on the sphere. The point corresponding to the lattice vector $\mathbf{G} = 1\mathbf{b}_1 + 1\mathbf{b}_2$, shown dashed in Fig. 3.12a, is found by rotating the lattice by an angle θ around the end point of $\mathbf{k}$, as shown in Fig 3.12b. A measurement is usually a stepwise scan along a line in reciprocal space, where the intensity is measured in each step.

Fig. 3.11b shows an SXRD scan along the h axis of a clean Rh surface. It reveals intensity peaks in $h = -1$ and $h = -2$, corresponding to the $(-1, 0)$ and $(-2, 0)$ CTRs respectively.

3.3 Scanning Tunneling Microscopy

Scanning Tunneling Microscopy (STM) was invented by Binning, Rohrer, Garber and Weibel in 1981 and has revolutionized the field of surface science as the first method for obtaining direct real-space images of surface structures on the atomic scale [39, 40]. Therefore STM is widely used and plays a crucial role in the studies reported in this thesis.

The main idea is that a very sharp metal tip is brought close enough to the surface, in order to allow for a significant tunneling of electrons through the vacuum gap inbetween (see Fig. 3.13a). By
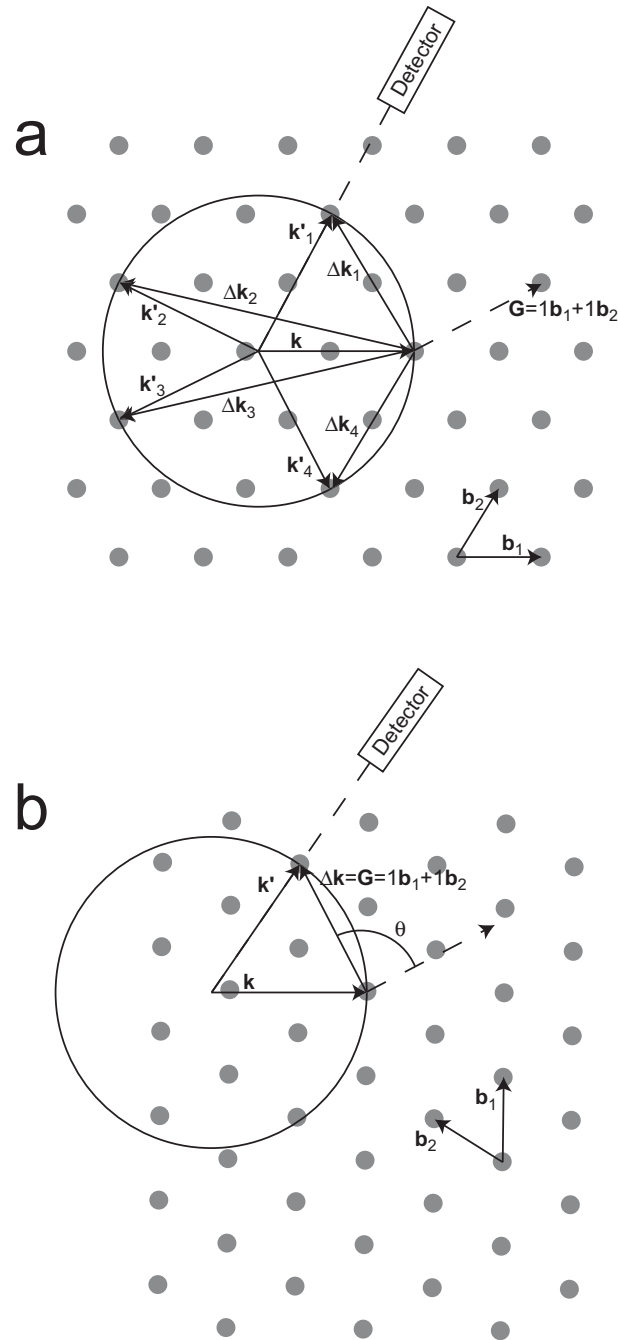
Figure 3.12: The Ewald sphere illustrating the diffraction measurement. a) The incoming wave vectors, $\mathbf{k}$, is drawn such that it points at a reciprocal lattice point and the outgoing lattice vector, $\mathbf{k}'$, is placed sharing the same starting point. $\mathbf{k}'$ can then reach the points in reciprocal space, that lie on a sphere of radius k around the starting point, and by placing a detector in the direction of $\mathbf{k}'$, the corresponding intensity can be measured. The momentum change $\mathbf{\Delta k}$ is shown as the vector between the endpoints of $\mathbf{k}$ and $\mathbf{k}'$, and in the case that $\mathbf{\Delta k}$ is a reciprocal lattice vector, constructive interference, and thus an intensity peak, is obtained. b) By rotating the the reciprocal space, other points coincide with the sphere and can be measured.